

1 **A novel index for the study of synergistic effects during the co-processing of coal and biomass**

2 Jumoke M. OLADEJO¹, Stephen Adegbite¹, Cheng Heng Pang², Hao Liu³, Ashak M. Parvez¹, Tao Wu^{2,4,*}

3 ¹ Department of Chemical and Environmental Engineering, The University of Nottingham Ningbo China, Ningbo
4 315100, China

5 ² Municipal Key Laboratory of Clean Energy Conversion Technologies, The University of Nottingham Ningbo
6 China, Ningbo 315100, China

7 ³ Department of Architecture and Built Environment, The University of Nottingham, Nottingham NG7 2RD, The
8 UK

9 ⁴ New Materials Institute, The University of Nottingham Ningbo China, Ningbo 315100, China

10 Corresponding author: tao.wu@nottingham.edu.cn

11

12 **Abstract**

13 In this study, synergistic interaction between coal and biomass and its intensity was
14 investigated systematically using a low rank coal and its blends with different biomass
15 samples at various blending ratios. The catalytic effects of minerals originated from biomass
16 were also studied. It was found that some of the minerals existing in the ash derived from
17 oat straw catalysed the combustions process and contributed to synergistic interactions.
18 However, for the coal and rice husk blends, minimal improvements were recorded even
19 when the biomass and coal blending ratio was as high as 30 wt%. Biomass volatile also
20 influenced the overall combustion performance of the blends and contributed to synergistic
21 interactions between the two fuels in the blends. Based on these findings, a novel index was
22 formulated to quantify the degree of synergistic interactions. This index was also validated
23 using data extracted from literature and showed high correlation coefficient. It was found
24 that at a blending ratio of 30 wt% of oat straw in the blend, the degree of synergistic
25 interaction between coal and oat straw showed an additional SF value of 0.25 with non-
26 catalytic and catalytic synergistic effect contributing 0.16 (64%) and 0.09 (36%) respectively.

27 This index could be used in the selection of right type of biomass and proper blending ratios
28 for co-firing at coal-fired power stations, which intend to improve combustion performance
29 of poor quality coal by enhancing synergistic interactions during co-processing.

30 Keywords – Fuel characterisation; synergistic interaction; performance index; synergy index;
31 thermogravimetric analysis

32 **1.0 Introduction**

33 The low cost and carbon lean nature of biomass make it a promising energy alternative for
34 the mitigation of CO₂ emissions [1, 2]. However, the technical, economic and socio-ethical
35 issues associated with the large-scale utilization of biomass have hindered its large-scale
36 development [3, 4]. One of the feasible solutions to mitigate these issues is to cofire
37 biomass with coal. This approach has become a general practice in western countries as it
38 offers significant social and environmental benefits such as energy security, energy
39 sustainability, greenhouse gas emission reduction, and economic developments [1].

40 In the past few decades, extensive research has been carried out in understanding the
41 suitability of coal/biomass blends in various thermochemical conversion processes [5-7].

42 Synergistic effect was observed for some blends [1, 8] while insignificant additive behaviour
43 was also observed for some other blends [9, 10]. The synergy observed in coal/biomass fuel
44 blends was mainly attributed to both catalytic and non-catalytic synergistic effect of
45 biomass constituents and their influence on the coal during co-firing. The non-catalytic
46 synergistic effect is mainly associated with the high volatile content in biomass while
47 catalytic synergistic effect is dictated by Alkali and Alkali Earth Metals (AAEMs) in biomass
48 which have catalytic impacts on the reactivity of chars derived from coal [11, 12].
49 Nonetheless, even though all biomass have AAEM species, the presence of synergy and its

50 intensity is dependent on the physical/chemical properties of the fuels, especially the AAEM
51 contents [13].

52 To date, much effort has been made to understand the influence of AAEMs on the catalytic
53 influence on co-processing of biomass with coal. Many researchers have studied the
54 catalytic performance of ash derived from high temperature ashing process ($\geq 550^\circ \text{C}$) or
55 some ash elements, such as K, Ca and Si [14]. However, some AAEM species are normally
56 released at very low temperatures ($<500^\circ \text{C}$) [15]. Therefore the use of high temperature ash
57 as catalyst did not show the catalytic effect of AAEMs originated from biomass. So far, not
58 much work has been carried out to show the catalytic effect of minerals in biomass. In
59 addition, although synergistic interactions [1, 8] have been studied greatly in the past few
60 decades, there is not much effort being made to distinguish the contribution of catalytic
61 effect and non-catalytic effect on the overall synergistic interactions occurring, needless to
62 say there is a reliable approach to quantify synergistic interactions and the contribution
63 from catalytic and non-catalytic factors.

64 This paper focuses on the synergistic interactions between coal and biomass in the blends.
65 Thermogravimetric analysis (TGA) was conducted to understand the catalytic effects of
66 minerals (AAEMs) from biomass and the non-catalytic effects of volatile matters on the co-
67 processing of biomass with coal. A novel indicator was therefore proposed to evaluate the
68 extent of synergistic interactions as well as to quantify the contribution of catalytic and non-
69 catalytic effects to these interactions.

70 **2.0 Experimental**

71 **2.1 Coal and Biomass Samples**

72 One coal and two types of biomass were used in this research. The coal, Yunnan (YC), was
73 obtained from Fuyuan town (Yunnan Province, China), which is mainly used for industrial
74 process heating especially in wine-making industry. The biomass samples, Oat Straw (OS)
75 and Rice Husk (RH), were chosen to represent agricultural waste and agro-industrial residue
76 respectively due to their abundance globally.

77 **2.1.1 Sample Preparation**

78 The samples were prepared following standard procedures described elsewhere (BS EN
79 14780 and ISO 13909) [16, 17]. All the samples were initially reduced to a size smaller than
80 500 μm using a cutting mill (Retsch SM 2000, Germany), and further milled to be smaller
81 than 106 μm using a Retsch SM 200 mill. Each biomass was blended with the coal in three
82 mass fractions, i.e., 10, 30 and 50 wt%.

83 **2.2 Proximate, Ultimate and Heating Value Analyses**

84 Proximate analysis was performed using the thermo-gravimetric analyser (TGA) (STA 449 F3
85 Netzsch, Germany) while ultimate analysis of the samples was conducted using a PE 2400
86 Series II CHNS/O Analyzer (PerkinElmer, USA). In a TGA test, approximately 5 –10 mg of the
87 sample was placed in an alumina crucible following a testing procedure described elsewhere
88 [18, 19] . For ultimate analysis, approximately 1.5 mg of sample was placed in a platinum foil
89 pan. The higher heating value (HHV) of a sample was measured using an IKA Calorimeter
90 C200 (IKA, USA), which utilized approximately 1.0 g of the sample. All experiments were
91 repeated at least three times with the average value used as the final value.

92 **2.3 Mineral Composition of Fuel**

93 Mineral composition of the unblended fuels was determined by using an X-ray Fluorescence
94 (XRF) spectrometer, the procedure adopted is described elsewhere [20].

95 **2.4 Thermal Analysis**

96 Combustion characteristics of individual fuels and their blends were measured following a
97 non-isothermal method, which was amended from elsewhere [21, 22]. In the test, the
98 sample was heated in air (80 vol% Nitrogen and 20 vol% Oxygen) from 50 to 900 °C at a
99 heating rate of 20 °C min⁻¹ and a gas flow rate of 50 ml min⁻¹. Characterisation of pyrolysis
100 was also conducted using the same technique under pure nitrogen atmosphere (>99.9%). All
101 experiments were repeated at least three times to ensure repeatability and accuracy.

102 The initiation temperature (IT) is the temperature at which 0.3 wt% mass loss rate of the
103 sample was achieved after the release of moisture, which is normally used as an indication
104 of the start of fuel decomposition. In fuel characterisation, the peak temperature (PT) is
105 considered inversely proportional to the reactivity/combustibility of the fuel, which was
106 determined as the temperature where the weight loss ($\frac{dw}{dt}$) of the sample reached its
107 maximum. The burnout temperature (BT) represents the end temperature of the burning
108 process, which was determined as the temperature when the rate of burnout (mass loss
109 rate) decreased to less than 1 wt% min⁻¹ on weight basis. The ignition temperature at which
110 the fuel burns spontaneously without external heat source was also obtained based on the
111 method adopted by many others [23].

112 **2.4 Performance Indices**

113 The ignition (Z_i) and combustion (S) index of the fuel and their blends were calculated based
114 on the Equations (1) and (2) [23].

115
$$Z_i = \frac{\left(\frac{dw}{dt}\right)_{\max}}{t_i t_{\max}} \times 10^2 \quad (1)$$

116
$$S = \frac{\left(\frac{dw}{dt}\right)_{\max} \left(\frac{dw}{dt}\right)_{\text{av}}}{T_i^2 T_b} \times 10^6 \quad (2)$$

117 Where:

118 $\left(\frac{dw}{dt}\right)_{\max}$ is the maximum rate of mass loss (% min⁻¹);

119 $\left(\frac{dw}{dt}\right)_{\text{av}}$ is the average rate of mass loss (% min⁻¹);

120 t_{\max} is the time at which the peak mass loss rate is attained (min);

121 t_i is the ignition time (min);

122 T_i is the ignition temperature (°C);

123 T_b is the burnout time (min).

124 **2.5 Low Temperature Ashing**

125 The low temperature ashing of biomass samples was performed using a PR300 Plasma
126 Cleaner (Yamato Scientific, Japan). This device was used to burn off the carbonaceous
127 components of the sample at low temperatures (less than 150°C) under which the presence
128 of minerals in biomass remains unchanged. The plasma was generated at a power of 200 W.
129 Approximately 0.5 g of a sample was loaded on a glass crucible, placed in the ashing
130 chamber, and exposed to pure oxygen at a flow rate of 100 ml min⁻¹ to ensure minimal
131 reflection of the plasma beam. Each ashing experiment required 30 hours for the complete
132 burning of carbonaceous materials.

133 **2.6 Catalytic Effect of Biomass-Derived Ash**

134 To understand the influence of minerals from biomass on combustion process, low
135 temperature ash of each biomass was blended with Yunnan coal at a blending ratio
136 equivalent to 30 wt% biomass in blend. The intrinsic reactivity of these blends was carried
137 out.

138 **3.0 Results and Discussion**

139 **3.1 Proximate, Ultimate and Heating Value Analyses**

140 Results of ultimate and proximate analyses of the samples are shown in Table 1. The coal
141 sample showed the highest heating value, which suggests that the blending of coal with
142 biomass of lower energy content would normally lead to the reduction in combustion
143 temperature in existing utility boilers [24]. The Rice Husk had very similar sulphur content
144 (0.4 wt%) but significantly different ash content (21.2 wt%) compared with Oat Straw. Oat
145 Straw had the highest volatile matter (72.1 wt%).

146 **Table 1 – Ultimate and proximate analysis of samples**

	Rice Husk (RH)	Oat Straw (OS)	Yunnan Coal (YC)
Ultimate analysis (wt%, daf)			
Carbon	50.1	47.5	86.2
Hydrogen	7.4	6.8	5.1
Nitrogen	1.7	2.3	1.0
Sulphur	0.4	0.3	1.1
Oxygen (by difference)	40.4	43.2	6.6
LHV (MJ Kg ⁻¹)	19.6	17.6	33.5
Proximate analysis (wt%)			
Moisture	4.1	4.0	4.5

Volatile Matter (VM)	62.8	72.1	27.2
Fixed Carbon (FC)	11.9	17.4	57.3
Ash	21.2	6.5	11

147 Mineral composition of the samples is illustrated in **Table 2**. The biomass samples had
148 relatively low sulphur content, which helps mitigate the environmental impacts associated
149 with the emission of sulphur oxides (SO_x). Normally, the reaction of AAEMs originating from
150 biomass with SO_x could lead to the formation of sulphates which contributes to the capture
151 of gas phase sulphur [25]. This is an important advantage of co-firing of coal with biomass,
152 especially for coals of relatively high sulphur content, such as Yunnan coal.

153 Normally, alkali metals, such as potassium (K) and sodium (Na), and alkali earth metals
154 (AAEMs), such as calcium (Ca) and magnesium (Mg), are known to have catalytic effect to
155 the thermal decomposition of fuels [26]. Table 2 shows the elemental composition of low
156 temperature ash derived from all samples studied. The OS, RH and YC had high AAEM of
157 61.6 wt%, 26.9 wt% and 25.5 wt% respectively. The high potassium content in the OS and
158 RH and the high content of calcium in YC suggest their likelihood of enhancing combustion
159 performance. Another interesting element that has been known to aid the release and
160 activation of these catalytic AAEMs is Cl, which was very high in OS (24.2 wt%) [27]. This
161 further supports the high potential in catalytic effect when OS is blended with YC. However,
162 it was reported that the enhancement could be weakened by the reaction between the
163 catalytic minerals, such as AAEMs, with silicates and/or alumina-silicates [28]. This means
164 that the high Si content in RH (45%) and YC (26.2%) might hinder the catalytic effects of
165 AAEMs. Nonetheless, the potential of enhanced catalytic effects of the YC and OS fuel
166 blends remained positive due to the high AAEM-to-Si ratio. However, the high Si content of

167 RH might still hinder such improvements for YC and RH blends. In addition, it must be noted
 168 that agglomeration and clinkering may arise when a biomass fuel has high Na and K
 169 contents as observed in OS due to the formation of sticky low temperature melts of silicate
 170 eutectics [29].

171 **Table 2 – Mineral composition of the samples (wt%)**

Elements	Rice Husk (RH)	Oat Straw (OS)	Yunnan Coal (YC)
Fe	5.4	1.5	21.0
K	20.2	47.4	4.8
Si	45.0	8.8	26.2
P	15.8	3.1	-
Ca	4.6	14.2	20.7
S	-	-	20.5
Cl	5.0	24.2	-
Na	0.6	-	-
Al	0.3	0.3	1.4
Ti		-	3.8
Mg	1.5	-	-
Mn	1.6	-	-
Br		0.4	1.6

172 **3.2 Intrinsic Reactivity**

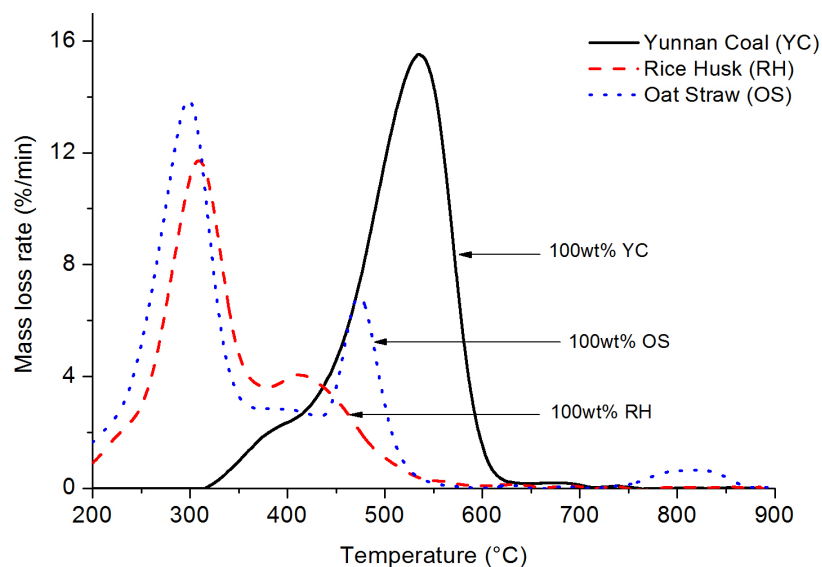
173 **3.2.1 Reactivity of Individual Fuels**

174 The thermal decomposition curves of OS, RH and YC is shown in Figure 1 with key features
 175 extracted and summarized in Table 3. It is evident that YC had one major decomposition
 176 stage with a strong peak for char burnout while the biomass samples were featured with
 177 two main mass loss stages representing the decomposition of organic compounds in the fuel.
 178 For the biomass samples, the first stage in the range of 144 – 420 °C represented the

179 decomposition of hemicellulose, cellulose and partial decomposition of lignin [30]. The
180 second stage represented mainly char burnout as well as the decomposition of lignin and
181 fell in the range of 378 - 518°C.

182 It is showed that the degradation of OS and RH began at 144 and 166 °C respectively. Both
183 samples exhibited an initial slow mass loss from initiation till about 255 °C due to the slow
184 decomposition of lignin content. When temperature was raised above this point, the mass
185 loss rate increased rapidly and reached the peak temperatures of 299 and 309 °C, for OS and
186 RH respectively, attributed mainly to the decomposition of hemicellulose and cellulose.

187 As shown in the DTG curve of RH, the mass loss rate increased immediately after the first
188 reaction zone, while for OS, a flat mass loss region was observed before the second reaction
189 zone which showed a sharp increase in DTG rate. This suggests a lower reactivity of the OS
190 char particles and higher mass loss rate at higher temperatures.



191

192

Figure 1: DTG curves oat straw, rice husk and Yunnan coal

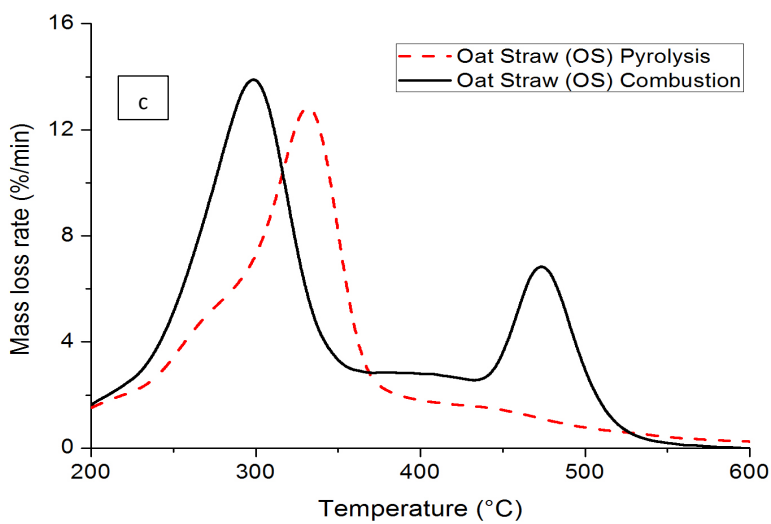
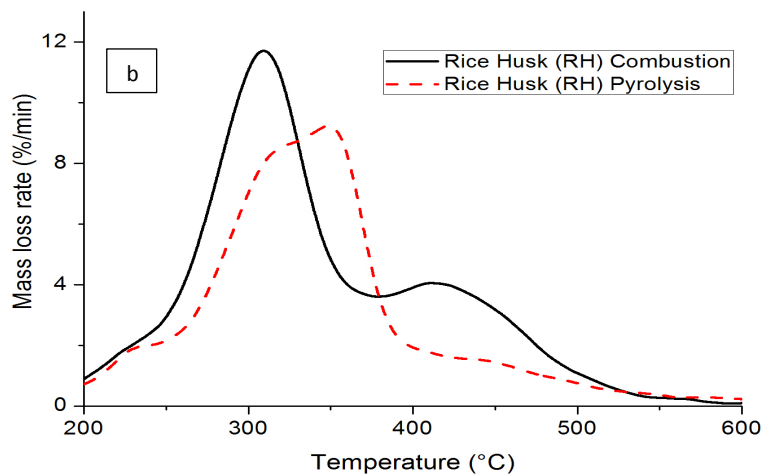
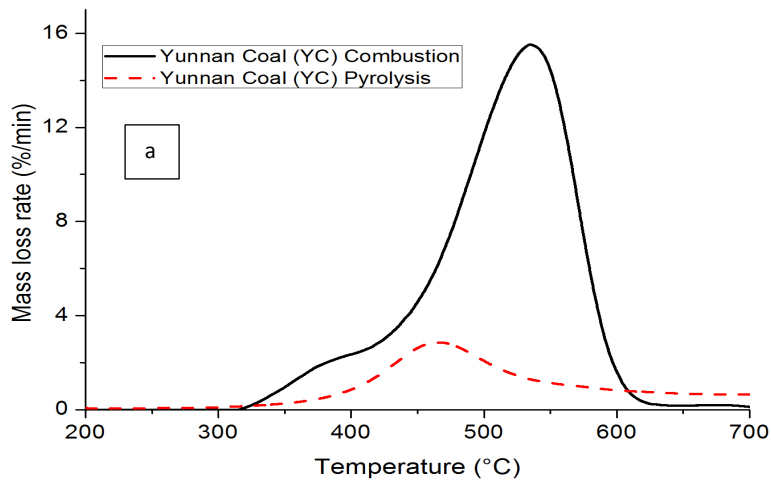
193 The difference in the 2nd stage reactivity could be linked to the catalytic influence of the
194 mineral contents of OS. It was found [31] that catalytic effect of potassium contributed to
195 the clear distinction of the two devolatilization peaks and shifted the first peak
196 temperature to a lower temperature. In this study, it is believed that the high potassium
197 content in OS (as shown in **Table 2**) enhanced the complete decomposition of lighter
198 volatile species and the release of more volatiles, which subsequently led to the formation
199 of more porous char with higher overall burnout reactivity.

200 YC decomposed at a temperature range between 329 and 605 °C with its only peak
201 appearing at 535 °C and exhibited a more synchronized mechanism of thermal
202 decomposition. In this study, the comparison of the combustion and pyrolysis profiles
203 showed that 83 wt% (RH) and 97 wt% (OS) of total volatiles in biomass samples were burnt
204 during the first reaction stage as an indication of its homogenous (gas-phase) ignition
205 mechanism. This is relatively unclear for YC due to its singular peak as its degradation curve
206 could be indicative of the simultaneous combustion of both volatiles and char over a wider
207 temperature range.

208 From the pyrolysis profiles shown in Figure 2, it is evident that the devolatilization of YC
209 occurred at higher temperatures (355 – 571 °C) compared with OS (146-489 °C) and RH (168
210 – 486 °C). The low pyrolysis rate and the high temperature required for YC could signify an
211 increase in resistivity of volatile release in the organic structure. The pyrolysis mass loss rate
212 of the biomass samples remained close to that of the combustion profile, which can be
213 explained by their high combustibility and reactivity of the volatile matter [32].

214 The decreasing peak temperatures of the biomass samples during combustion as shown in
215 Figures 2b-c suggested the enhanced reactivity during combustion compared with pyrolysis.

216 However this reduction in the peak temperature is not obvious in Figure 2a because of its
217 low volatile content of YC.



221 **Figure 2: Pyrolysis and combustion profiles of (a) Yunnan coal, (b) Rice Husk, and, (c) Oat**
 222 **Straw**

223 Normally, higher oxygen content of the biomass samples is an indicator of their high
 224 reactivity [33]. Among these three fuels studied, the most reactive fuel is OS with oxygen
 225 content of 43.2 wt% as shown in **Table 1**. The high oxygen content and high oxygen/carbon
 226 ratio led to the formation of char with higher reactivity [19]. Likewise, the high volatile and
 227 low fixed carbon content of biomass resulted in the yield of a small amount of highly porous
 228 char, which subsequently contributed to the high overall reactivity of the fuel.

229 For RH, OS and YC, the ratio of volatile matter to fixed carbon, another indicator of
 230 combustion reactivity, is 5.3, 4.2 and 0.48 respectively. This ratio is an indicator of the fuel's
 231 volatility, a ratio >4 suggests homogenous oxidation of the volatiles while a ratio smaller
 232 than 1 indicates heterogeneous gas-solid reactions [22]. Therefore, the combustion of RH
 233 and OS was predominantly the gaseous phase oxidation of its volatiles while for YC it was
 234 the simultaneous oxidation of both volatiles and char.

235 **Table 3 – Combustion characteristics of Rice husk, Yunnan coal and their blends**

Property		RH	50 wt%YC+ 50 wt%RH	70 wt%YC+ 30 wt% RH	90 wt%YC+ 10 wt%RH	YC
Initiation Temperature (°C)		166	192	222	222	329
Zone	Temperature range (°C)	166 - 370	192 - 369	222 - 356	286 - 608	329 - 605
	Peak Temperature (°C)	309	308	313	532	535

	Total mass loss (wt%)	49.3	24.4	13.1	85	88
	Average mass loss rate (wt% min ⁻¹)	4.8	2.8	1.9	5.3	6.4
	Maximum mass loss rate (wt% min ⁻¹)	11.7	4.9	3.2	13.4	15.5
Second Reaction Zone	Temperature range (°C)	378 - 503	378 - 601	364 - 601		
	Peak Temperature (°C)	411	519	531		
	Total mass loss (wt%)	18.8	53	66.5		
	Average mass loss rate (wt% min ⁻¹)	3	4.8	5.6		
	Maximum mass loss rate (wt% min ⁻¹)	4.1	7.8	11.1		
	Burnout Temperature (°C)	503	601	601	608	605
	Residual Weight at burnout (wt%)	26.7	18.4	16.5	13.1	11.9

236

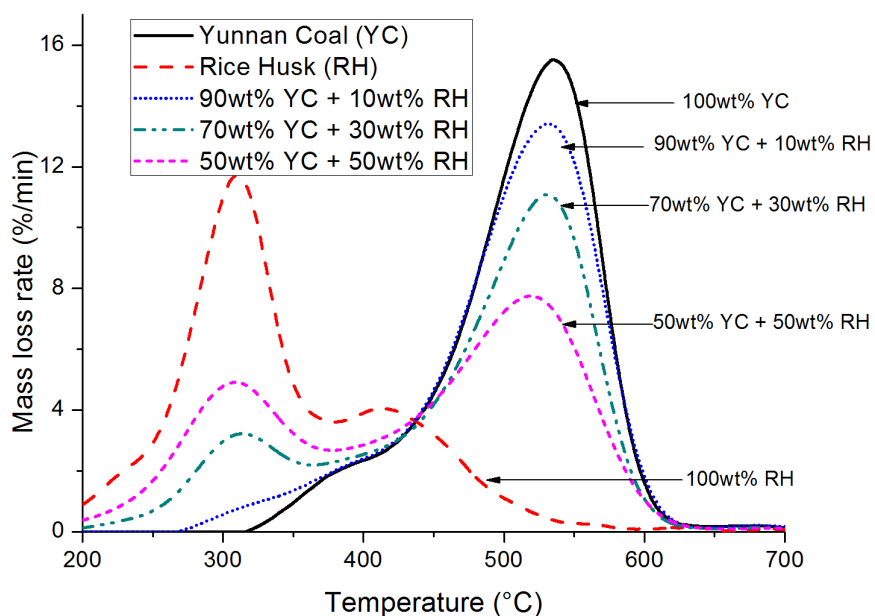
Table 4 – Combustion characteristics of Oat straw, Yunnan coal and their blends

	OS	50 wt%YC+ 50 wt%OS	70 wt%YC+ 30 wt%OS	90 wt%YC+ 10 wt%OS	YC	
Initiation Temperature (°C)	144	162	201	244	329	
First Reaction Zone	Temperature range (°C)	144 - 420	162 - 346	201 - 345	244 - 334	329 - 605
	Peak Temperature (°C)	299	299	301	305	535
	Total mass loss (wt%)	65	27.4	13.1	6	88
	Average mass loss rate	4.7	3	1.8	1.3	6.4

Second Reaction Zone	(wt% min ⁻¹)					
	Maximum mass loss rate (wt% min ⁻¹)	13.9	7.2	2.9	1.8	15.5
	Temperature range (°C)	432 - 518	349 - 564	353 - 583	339 - 591	
	Peak Temperature (°C)	474	456	483	515	
	Total mass loss (wt%)	17.6	58.1	68.7	79.9	
	Average mass loss rate (wt% min ⁻¹)	4.1	5.4	5.9	6.3	
	Maximum mass loss rate (wt% min ⁻¹)	6.8	8.7	11.1	13.9	
	Burnout Temperature (°C)	518	564	583	591	605
	Residual Weight at burnout (wt%)	11.8	11.2	14.2	10.5	11.9

237 **3.2.2 Combustion Characteristics of the Blends**

238 Combustion characteristics of the YC/RH blends are presented in Figure 3 and Table 3.



239

240

Figure 3: DTG curve of Yunnan coal/Rice husk blends

241 Generally speaking, the blends featured two peaks. However, the first peak was not fully
242 developed for the blend with 10 wt% RH. As previously described by others [34], the first
243 peak temperature of the blend was similar to the first peak temperature of the biomass, i.e.
244 rice husk (309°C), while the second peak temperature and burnout temperature were
245 similar to the peak (535 °C) and burnout temperatures (605 °C) of the Yunnan Coal with
246 minimal deviations. The maximum rate of degradation of the first peak increased with the
247 increase in the RH, while for the second stage, the rate reduced with the increase in RH. This
248 occurrence was due to the combustion of biomass volatiles prevailing in the first reaction
249 zone, while the coal char burning dominated the second reaction zone [35]. It was also
250 observed that the residual weight at burnout temperature increased with the increase in RH
251 due to the high ash content, which might present extra barrier for heat and mass transfer.

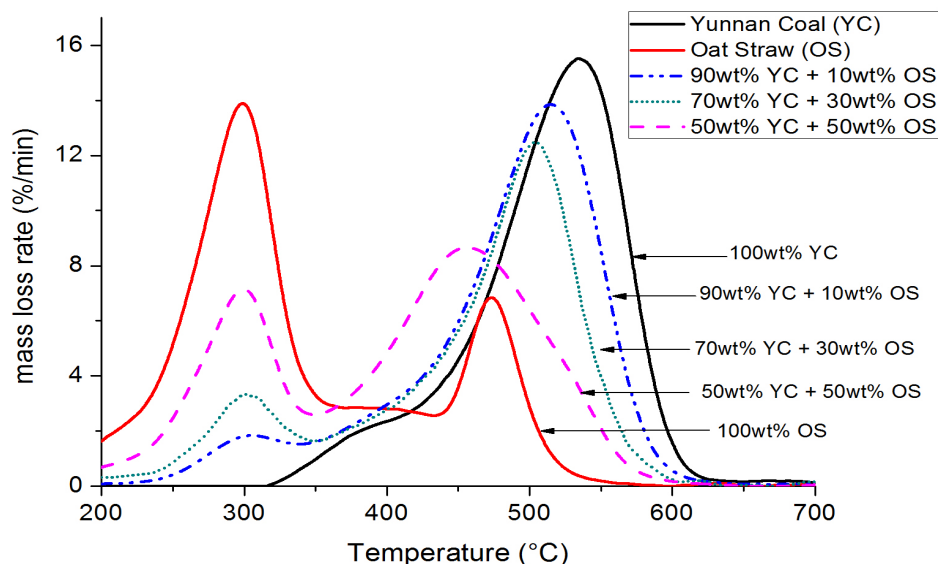
252 Similar to YC/RH blends, the YC/OS blends, as shown in Figure 4 and Table 2, had two distinct
253 peaks. However, there was a noticeable decrease in the peak temperature with the increase
254 in oat straw. Since the peak and burnout temperature of OS were lower than those of YC.
255 This reduction in the 2nd peak temperature indicated improved combustion reactivity as a
256 result of synergistic interactions between coal and biomass as shown in in Figure 4b. To
257 further prove the presence of synergy, the experimental results were compared with the
258 theoretical values calculated using the weighted sum of the pure feedstock [36]. The result
259 obtained for the oat straw blend showed distinct shift of the 2nd reaction stage towards
260 lower temperatures compared with theoretical values. However, the theoretical and
261 experimental values of rice husk blends were similar when the blending ratio was below 30
262 wt%, while for 50 wt%, the shift towards lower temperatures did become noticeable.

263 Synergistic interactions can be associated with catalytic and/or non-catalytic mechanisms.
264 The latter involves the formation of free radicals and hydrogen transfer from biomass to coal
265 while the former is based on catalytic effect of alkali and alkali earth metals present in
266 biomass or coal [37]. Consequently, the synergy observed in YC/OS blends could be partially
267 attributed to the catalytic effect of mineral matters in oat straw due to its high alkali metal
268 content, a common occurrence in herbaceous biomass [14, 31, 38]. This could be
269 supplemented by the non-catalytic improvement caused by the interactions of biomass
270 volatiles with coal char as well as the differences in morphology [39]. The release of volatiles
271 from biomass could result in the formation of free radicals during thermal reaction to
272 promote the breakdown of the dense and heat-resistive coal structural components
273 (polycyclic aromatic hydrocarbon bonded by aromatic rings) at lower temperatures [40, 41].
274 Therefore, the higher hydrogen-carbon mole ratio (H/C) of biomass in blends contributed to
275 the improvements observed in coal decomposition [42, 43]. The existence of synergy was
276 quite contentious, as synergistic interaction is not observed in all coal/biomass blends in the
277 first place. However synergistic enhancement was observed in coal and biomass fuel blends
278 even after the demineralisation of its biomass, eliminating catalytic effect of ash as the only
279 cause of synergy [31].

280 At low blending ratios, such as 10 wt% to 30 wt%, peak temperature of each reaction zone
281 was dominated by the fuel fraction with the higher mass loss. This mechanism of
282 decomposition is an indication of independent decomposition of both fuels, which suggests
283 the additive behaviours instead of synergistic interactions between YC and RH, which is
284 similar to what was reported by others [44]. However, slight reduction in the peak
285 temperature of the second reaction zone was observed in the 50 wt% RH blend, which

286 suggested some interactions between YC and RH. This can only be attributed to the increase
287 in volatiles available from 50% RH and its impacts on non-catalytic synergy mechanism.

288



289

290 Figure 4: DTG curve of Yunnan coal /oat straw blends

291 Taking into account the findings for both biomass blends, it can be concluded that the
292 presence of synergy, its extent and the mechanism are dependent on biomass types,
293 blending ratio and properties.

294 3.3 Ignition Temperature

295 The ignition temperatures (T_i) of the fuels are shown in Table 5, which were determined
296 following the method described elsewhere [8]. The ease of ignition of the biomass samples
297 is a consequence of their high volatile content (>80 wt%) as shown in Table 1. The ignition
298 temperature of YC was almost 200 °C higher than those of the biomass samples, which
299 might be due to the hetero-homogeneous ignition mode of this coal [11].

300 However the main mass loss of the blends was characterised by the 2nd peak temperature,
 301 which more accurately depicted the effect of biomass addition on the oxidation of coal.
 302 Hence, a “trigger temperature” was also extracted from the TGA profiles for the 2nd reaction
 303 stage to characterise the ignition of the char oxidation, which is the temperature
 304 corresponding to the intersection of the tangent line of the initial mass loss curve (before
 305 the sharp drop in mass) and the tangent line that is drawn at the intersection of the vertical
 306 line through the 2nd Peak temperature and the mass loss curve [23].

307 The ignition points of YC/RH and YC/OS blends were slightly higher (<20 °C) than the ignition
 308 temperature of the OS (256 °C) and RH (266 °C) in the blend. This suggests weak interactions
 309 between fuels in the blends. The 10 wt% RH blend remained close to the ignition
 310 temperature of YC due to the immature first peak as seen in Figure 3a. However, the trigger
 311 temperatures reduced significantly compared with that of YC (459 °C). The changes in
 312 trigger temperature with blending ratio are shown in Figure 5 with the dotted lines
 313 representing predictions based on additive behaviours. The blends exhibited a slow drop
 314 between 10 and 30 wt%, followed by a sharp drop in this temperature between the 30 and
 315 50 wt%. The 50 wt% OS blends exhibited the largest temperature decrease. These changes
 316 in ignition parameter are the result of interactions between individual fuels in the blends.

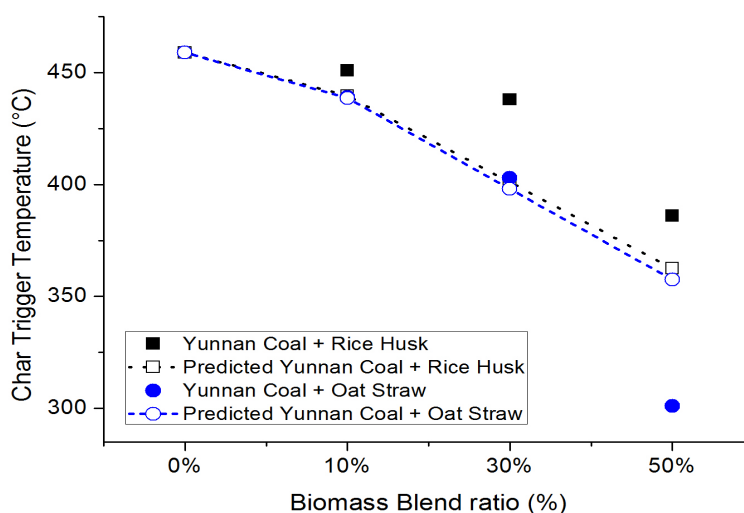
317 **Table 5 – Ignition temperature of individual fuels and their blends**

Sample	Main Ignition Temperature (°C)	Char Trigger Temperature (°C)
100%RH	266	
90 wt% YC+10 wt% RH	451	451
70wt% YC+30 wt% RH	272	438
50 wt% YC+50 wt% RH	268	386

100%OS	256	
90 wt% YC+10 wt% OS	271	439
70 wt% YC+30 wt% OS	256	403
50 wt% YC +50 wt% OS	259	301
100 % YC	459	

318 The char trigger temperatures were also compared with theoretical values calculated from
319 ignition temperatures of the parent fuels assuming that additive property applies. These
320 calculated values are presented as the dashed lines in Figure 5. For YC/RH blends, the actual
321 trigger temperature was higher than predicted values. For YC/OS blends, the change of
322 trigger temperature of 10-30 wt% blends were relatively linear while for the 50 wt% blend,
323 it exhibited some improvements and lead to a lower temperature.

324 The changes in the ignition and char trigger temperatures were believed to be the
325 consequence of the interactions between the organic elements of the different fuels in the
326 blend [8, 23]. This non-catalytic synergy might be linked to the increase in volatile matter
327 content of the blends due to biomass addition.



328

329 **Figure 5: Evaluating additive trend in second reaction zone trigger temperature**

330 To quantify the influence of blending on ignition and combustion performance, the ignition
 331 (Z_i) and combustion (S) index of individual fuels and their blends were calculated using
 332 Equations (1) and (2) and are presented in Table 6. As shown in Table 6, OS showed the best
 333 ignition property while YC was the most difficult to ignite. The ignition index increased with
 334 the increase in biomass percentage for all oat straw blends and the 30 wt% RH blend, this is
 335 in line with the decrease in ignition temperature and ignition time. This suggests that the
 336 ignition properties of Yunnan coal were improved by blending with oat straw or rice husk at
 337 certain blending ratios due to the interaction between the fuels. However, insignificant
 338 improvement in ignition index was observed for 10 wt% and 50 wt% RH blends.

339 As can be seen in Equation (2), the combustion index was dependent on peak mass loss rate,
 340 peak and Ignition time; hence for the 10 wt% RH blend, it had similar ignition and peak time
 341 with YC. However, the peak mass loss rate was reduced. Similarly, the reduction in the peak
 342 mass loss rate of the 2nd reaction zone of the 50 wt% RH blend hindered the increase in the
 343 ignition index. In comparison to the OS blend, this trend for RH blends could be associated
 344 with the high ash content of RH, which reduced the amount of organic matter available for
 345 interaction with YC. It can be seen that among the blends, the 10 wt% OS blend had the best
 346 ignition index while the 10 wt% RH blend had the worst. This is consistent with what was
 347 found for coal and tobacco residues blends, a nearly linear increase in ignition index with
 348 increase in biomass due to the high volatile content of the biomass [53].

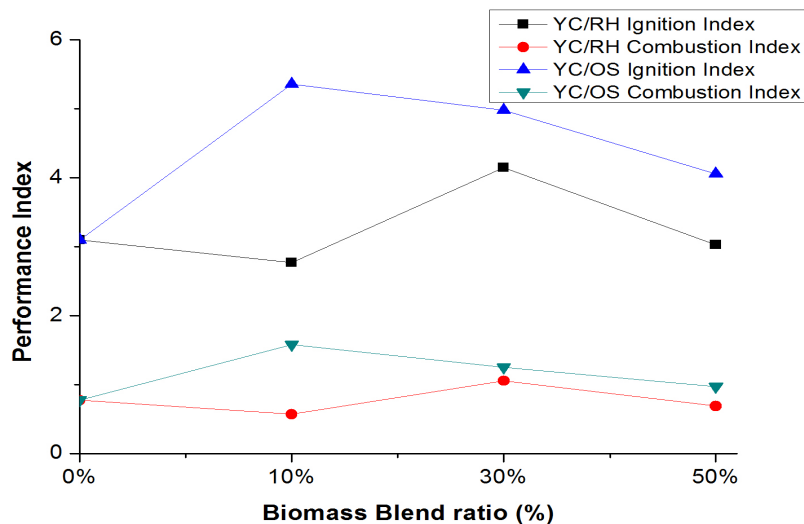
349 Table 6 – Performance Parameters of Individual fuels and their blends

	RH	OS	YC	90% YC+10 wt% RH	70% YC+30 wt% RH	50 wt% YC+ 50 wt% RH	90% YC+10 wt% OS	70% YC+30 wt% OS	50 wt% YC+ 50 wt% OS
Z_i (%/min ³)	8.4	10.9	3.1	2.8	4.2	3.0	5.4	5.0	4.1
S	1.4	1.8	0.8	0.6	1.1	0.7	1.6	1.2	1.0

(%/°C ³ min ²)								
---------------------------------------	--	--	--	--	--	--	--	--

350 The combustion index also suggested that OS was the most reactive. Improvement in
351 combustion performance was observed for the 30 wt% RH and all YC/OS blends. The
352 reduction in combustion index observed in the 10 wt% RH blend can be explained by
353 Equation (2). As mentioned earlier, the 10 wt% RH blend was featured with a single reaction
354 stage at 286 – 608 °C. This indicates a longer residence time required for attaining a desired
355 burnout in comparison with Yunnan coal which burnt out completely between 329 – 605 °C.
356 This suggests the absence of improvement in the combustion performance for 10 wt% RH in
357 comparison with Yunnan Coal. The reductions in the maximum (7.8 wt% min⁻¹) and average
358 mass loss rate (3.8 wt% min⁻¹) of the 50 wt% RH blend due to its double peaks could be
359 interpreted as a reduction in the overall fuel reactivity if this combustion index was used for
360 comparison. This is explained by the high value of the mass loss rates for YC with a peak of
361 15.5 wt% min⁻¹ and a mean mass loss of 6.4 wt% min⁻¹.

362 Normally, the combustibility of any fuel is inversely proportional to the maximum
363 decomposition rate temperature [45]. Similarly, the decrease in the 2nd peak temperature of
364 the OS blends illustrated an improvement in combustion performance. The enhancement in
365 the burnout of the fuels was represented by the small decrease in the burnout
366 temperatures with the maximum decrease of 6.7% for the 50 wt% OS blend, which is
367 consistent with what was reported by many others [34, 46].



368

369

Figure 6: Changes in performance index of fuel blends

370

Although the combustion and ignition indices (as shown in Figure 6) can be used to show

371

the interactions between individual fuels during co-processing, the accuracy of these indices

372

may be compromised due to the split of the weight loss into two reaction zones as the

373

average and maximum weight loss reduces more rapidly with the increase in blending ratio

374

compared with time and temperature. Therefore, there is a need to develop a novel index

375

to take into account the two reaction zones or the reaction zone exhibiting more synergistic

376

characteristics, thereby improve its reliability and ensure the results are representative of

377

the entire combustion process.

378 3.4 Catalytic Effect of Biomass Minerals

379

In this study, the influence of the minerals from biomass on the co-combustion

380

characteristics of the blends was studied. Low temperature ash of Oat Straw and Rice husk

381

were blended with YC to compare with the curve obtained for 30 wt% biomass and 70 wt%

382

YC, as shown in Figure 7 and Table 7. The 70 wt% YC and 30 wt% biomass was chosen as a

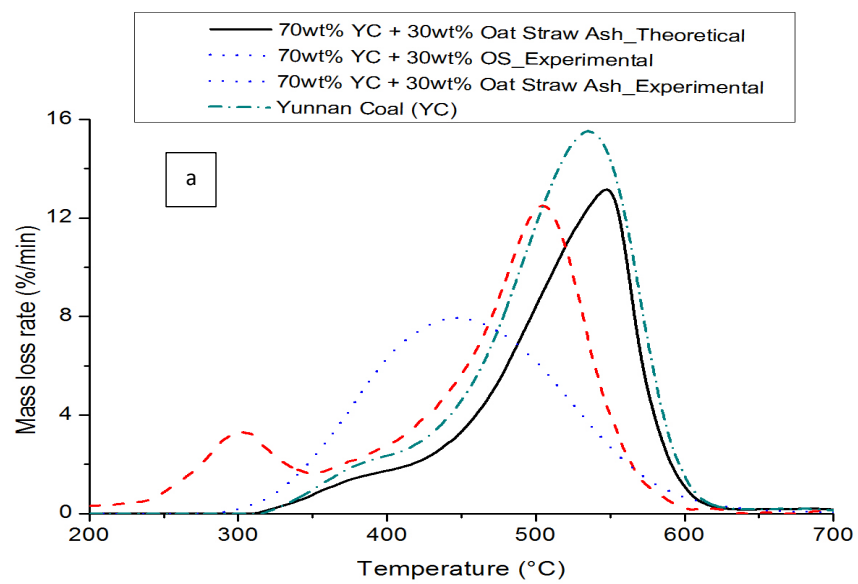
383

reference due to the improvement in ignition and combustion index were noticed in the

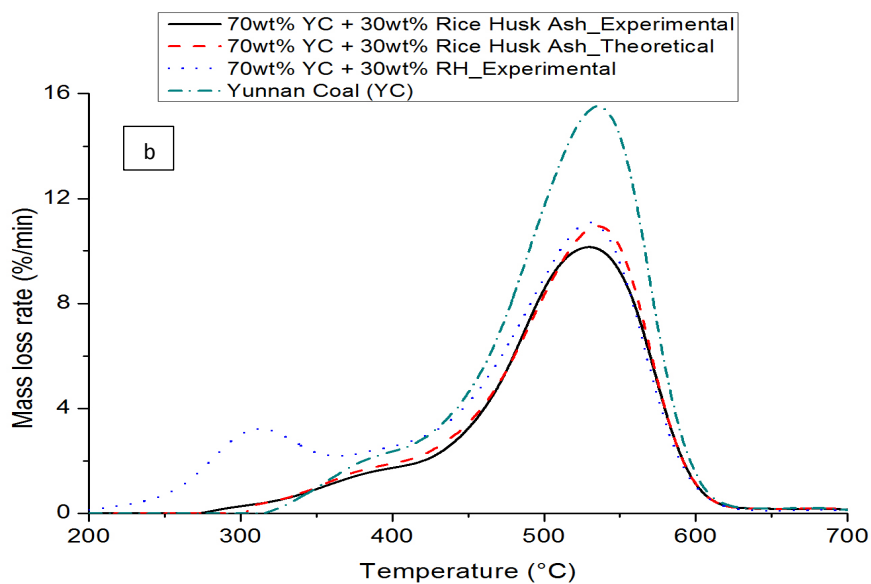
384

performance index for both YC/OS and YC/RH blends (as illustrated in Figure 6).

385 The results clearly showed changes in the characteristics of the 30 wt% OS ash blend which
 386 led to a lower ignition temperature of 403 °C, a lower peak temperature of 486 °C and a
 387 lower burnout temperature of 575 °C compared with those of 100% YC. The PT and BT vary
 388 significantly from the additive data.



389



390

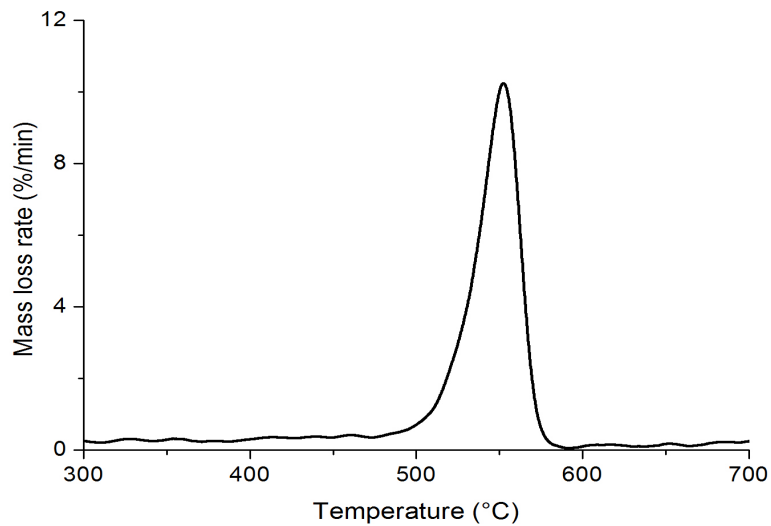
391 Figure 7: DTG curves of experimental and theoretical data of 100% YC and (a) 30 wt% Oat
 392 Straw ash & 30 wt% Oat Straw; (b) 30 wt% Rice Husk ash & 30 wt% Rice Husk

393 The variations in the ignition, peak and burnout temperatures could be explained to some
394 extent by the catalytic effect of the AAEMs originated from biomass such as Oat Straw. The
395 catalytic effect of AAEMs was found to be in order of Na > K > Ca [47]. As shown in **Table 2**
396 OS contained significant amount of AAEMs, which was greater than that of RH. The
397 investigation on the thermal behaviour of the low temperature ash derived from Oat Straw
398 (as illustrated in Figure 8) showed a mass loss of 17.6 wt% in a temperature range of 473-
399 573 °C, which peaked at 552 °C. This mass loss was attributed mainly to the release of
400 volatile AAEMs compounds at high temperatures such as K⁺, KCl and or KOH. The initial
401 volatile inorganic release temperature (552 °C) is lower than the burnout temperature of OS
402 (518 °C), which suggests that AAEMs acted as catalyst for the burnout of OS. Even at a
403 temperature higher than 573°C, there was still significant amount of AAEMs remaining as
404 catalyst for YC char combustion (burnout temperature is 605 °C) as only 17.6 wt% mass loss
405 upon heating while the initial mass fraction of potassium for OS low temperature ash was
406 47.4 wt% (as shown in **Table 2**). This is consistent with what was reported [15] that the
407 release of a small fraction (<20 wt%) of the organically bonded alkali metals occurred at
408 temperatures up to 800 °C. In this study, the high potassium and calcium content in OS
409 explains the reduction in the burnout temperature of 30 wt% Oat Straw ash blend from 605
410 to 575 °C. This reduction in burnout temperature was also evident in all the YC/OS blends.
411 The high AAEMs content in both OS and RH contributed to the reduction in char burnout
412 temperature of the fuel blends.

413 **Table 7 – Combustion characteristics of YC blended with low temperature ash of biomass**

Sample	Ignition Temp (°C)	Peak Temp (°C)	Total degradation (wt%)	Average degradation (wt%/min)	Maximum degradation rate (wt%/min)	Burnout Temp (°C)
--------	--------------------------	----------------------	-------------------------------	-------------------------------------	--	-------------------------

Yunnan Coal	459	535	88	6.4	15.5	605
70%YC + 30 wt% Rice Husk ash	454	529	61.7	4.2	10.1	601
70%YC + 30 wt% Oat Straw ash	403	486	64.2	5.2	10.0	575



414

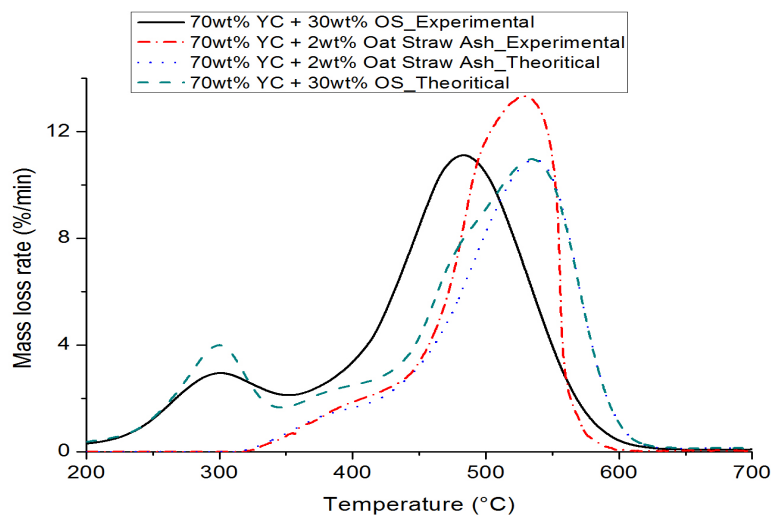
415

Figure 8: DTG of Oat Straw low Temperature ash

416 The peak temperature and burnout temperature of the 30 wt% RH Ash blend was
 417 comparable with that of 100 wt% YC. Likewise, the ignition temperature of the 30 wt% RH
 418 ash blend was similar to that of 100 wt% YC. This confirmed the absence of catalytic
 419 improvement when YC was blended with RH ash. Therefore, the synergistic interactions
 420 observed for RH (reductions in trigger temperature as shown in Table 3) could not be
 421 attributed to catalytic synergy for RH and are closely related to non-catalytic effects
 422 primarily linked to high volatile content and subsequently high char porosity.

423 Nonetheless, results of the 30wt% oat straw and coal blend did not distinguish the effect of
 424 volatiles and minerals although it proved the existence of strong synergy between the two
 425 fuels. Therefore, ash derived from oat straw (equivalent to 2 wt% ash) was used to reveal

426 the influence of minerals originated from oat straw on co-firing. A PT of 528 °C and a BT of
427 588 °C were observed as shown in Figure 9, which were 7 °C and 17 °C lower than those of
428 the coal respectively. This demonstrated a modest catalytic of the minerals in oat straw. As
429 previously mentioned, the PT and BT were 483 °C and 583 °C respectively for the 30 wt% OS
430 blend, it can therefore be concluded that for 30 wt% OS blend, the significant synergistic
431 effect could be attributed to the non-catalytic synergy by the organic content of the oat
432 straw and the catalytic activity of ash.



433

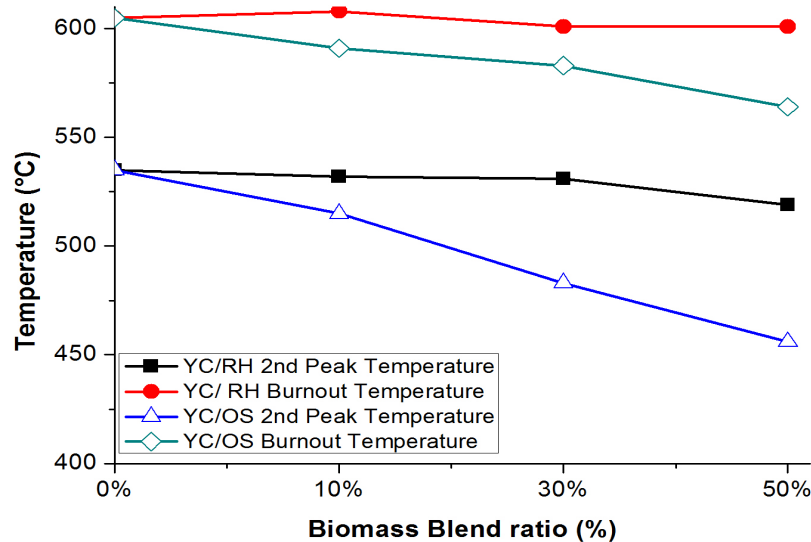
434 **Figure 9: DTG of experimental and theoretical 30wt% oat straw and 2wt% oat straw ash**
435 **blend**

436 3.5 Synergy Indicator

437 In this study, it is clear that factors, such as biomass blending ratio, biomass ash properties,
438 volatile content, contributed to strong synergistic interactions between coal and biomass.
439 Each factor affects the synergy observed in the blends to some degree. To select proper
440 biomass for co-processing with coal and to determine the proper blending ratio to enhance
441 synergistic interaction and therefore improve overall combustion performance, there is a

442 need to develop a novel index, which can also be used to evaluate the different impacts of
443 catalytic and non-catalytic effects.

444 Synergy index [48] proposed by others was solely a function of the reaction time to reach 95%
445 conversion where larger magnitude of the index indicates greater degree of synergy. In this
446 study, it is clear that the main synergistic improvement include the reduced 2nd peak and
447 burnout temperatures, as shown in the line chart in Figure 10. These observations have
448 been linked partially to the catalytic effects of biomass inorganic content as described in
449 section 3.4 and secondarily, to the non-catalytic effects of biomass organics (high volatiles
450 and char structure). Therefore, the three characteristic factors, i.e., peak temperature,
451 burnout temperature and time to peak of the second reaction stage, which have direct
452 influence on combustion performance, are used as the parameters for the novel synergy
453 index.



454
455 Figure 10: Improvements in peak and burnout temperatures with biomass blending

456 Consequently, the extent of synergistic interaction between the coal and biomass fuel can
457 be quantified by the formulation of a synergy factor (SF) based on the peak and burnout

458 temperatures of the second reaction zone as well as the time taken. In this study, a novel
459 synergy factor was developed, which is expressed as Equations (3).

$$460 \quad SF = \frac{SI_{blend}}{SI_{coal}} \quad (3)$$

461 Where SI is a synergy indicator ($^{\circ}\text{C}^{-3} \text{ min}^{-1/2}$) and can be calculated using Equation (4):

$$462 \quad SI = \frac{1}{t_{p-s} \cdot 0.5 T_b^2 T_p} \times 10^6 \quad (4)$$

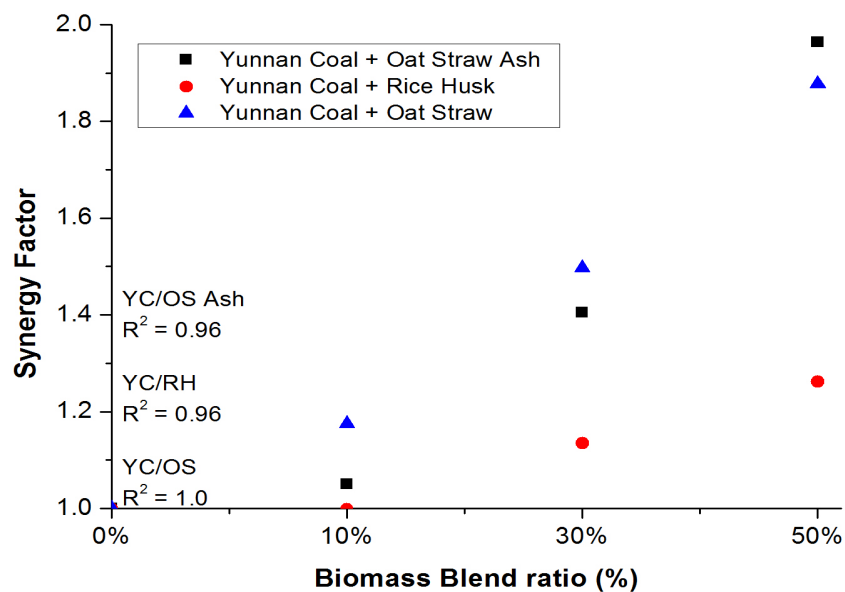
463 Where, t_{p-s} is the time difference between the start and peak of the second reaction zone
464 (min); T_p is the peak temperature ($^{\circ}\text{C}$); T_b is the burnout temperature ($^{\circ}\text{C}$).

465 Using this index, a comparison baseline was created using the result extracted from the
466 theoretical blends models to determine whether fuel blend establishes a more synergistic
467 effect ($SF > 1.15$) or additive behaviour ($0.8 \leq SF \leq 1.15$). However, a value of $SF \leq 0.8$
468 suggests deteriorated combustion performance after blending. The synergy factors for the
469 Yunnan coal and biomass blends discussed above are shown in Figure 11.

470 It can be seen that the synergy factor increased with the increase in blending ratio; however
471 the rate of increase with biomass blend ratio were different for different blends. For the 30
472 wt% biomass blends (as shown in Figure 6), the most significant synergistic effect occurred
473 for 70 wt% Yunnan coal + 30 wt% oat straw with a synergy factor of 1.50. The 70 wt%
474 Yunnan coal + 30 wt% rice husk blend showed additive behaviour and had an SF of 1.13. For
475 the 10 wt% biomass blends, the YC/RH blend exhibited additive behaviour, which was
476 mainly due to the insufficient amount of AAEMs to catalyse combustion process. Based on
477 these results, it can be concluded that for blends with 30 wt% of biomass, oat straw showed
478 more significantly enhanced reactivity than that of rice husk. The high SF of the 50% OS ash

479 blend was due to the existence of significant amount of catalytic species resulting in greater
 480 enhancement in combustion.

481 In this study, assuming an additive behaviour, for 70% YC and 30 wt% OS , the SF is of a
 482 value of 1.15. The SF of 70 wt% YC and 2 wt% OS ash was found to be 1.24, which suggests
 483 that catalytic synergy resulted in a SF change by 0.09. The difference between the SF value
 484 (S.F = 1.40) of 70% YC and 30 wt% OS and that of 70 wt% YC and 2 wt% OS ash (SF = 1.24)
 485 could be attributed to volatile effect (non-catalytic synergy) and resulted in a SF change of
 486 0.16. Likewise, the non-catalytic synergy detected in the 50wt% RH blend (SF = 1.26) could
 487 be attributed to its volatile content, which affected reaction time, and characteristic
 488 temperature at higher blend ratio, and resulted in an increase in SF by 0.11 due to non-
 489 catalytic synergy.



490

491

Figure 11: The Synergy indicator of Yunnan coal blends

492

Table 8 – Validation of Synergy Factors using Reported Data

		Biomass blending ratio / Synergy Factor

	Biomass types	0%	10%	30%	50%
Australian Coal (AC) blends[49]	Gumwood (GW)	1.00	1.19	1.27	1.43
	Poplar (PP)	1.00	1.16	1.26	1.38
	Rosewood (RW)	1.00	1.18	1.34	1.57
Mengxi Coal (MC) blends[49]	Gumwood (GW)	1.00	1.18	1.35	1.41
	Poplar (PP)	1.00	1.26	1.39	1.38
	Rosewood (RW)	1.00	1.31	1.80	1.67
Australian Coal (AC) blends [50]	Oat Straw (OS)	1.00	1.11	1.36	
	Printed circuit board (PCB)	1.00	1.03	1.23	
	Rubber	1.00	0.95	1.02	
	Polystyrene (PS)	1.00	1.39	1.40	

493 Figure 11 shows the synergy factor as a function of the biomass content of the blend
494 (regression function R^2 value ≥ 0.96). This is in line with past notions that the synergistic
495 interaction that occurred in fuel blends is a function of the organic and inorganic content of
496 the biomass, hence proportional to the portion of biomass introduced into the blend.
497 Nonetheless, the extent of enhancement remained dependent on the constituents of the
498 biomass sample used.

499 In order to verify this index, combustion data of Australian and Mengxi coal with biomass
500 blends were collated from literature [49, 50], which are illustrated in Table 8. Based on the
501 SF values, for all coal and biomass blends, significant synergistic interactions exist. As for
502 Australian Coal and Rubber, due to the lack of AAEMs in Rubber, which led to lack of
503 catalytic effects for combustion process, there was no noticeable synergistic effects
504 ($SF < 1.15$) being observed. However, for Australian Coal and PCB blends, at high blending
505 ratio, catalytic effects became obvious, which led to significant synergistic interactions
506 ($SF > 1.15$) at higher blending ratios (30 wt%). These findings are consistent with what the

507 authors found in their study and therefore proved the validity of the synergy factor
508 proposed in this study.

509 It was also reported [14] that the presence of an optimal improvement level for all fuel
510 blends, beyond which synergy was independent of the biomass blending ratio, which
511 suggests that the improvement of the blended fuels might plateau or even decrease after
512 certain blending ratio [14]. This is also confirmed by the lower SF values for 50 wt% Poplar
513 /MC and 50 % Rosewood/MC blends compared with the blends with only 30 wt% of
514 biomass

515 **4.0 Conclusions .**

516 In this study, the co-firing of Yunnan coal with AAEMs-rich Oat Straw demonstrated strong
517 synergistic interaction by the reductions in 2nd Peak and burnout temperatures. It is found
518 that AAEMs from biomass acted as catalysts for coal combustion, enabling catalytic synergy,
519 which is biomass dependent. Non-catalytic synergistic interactions were also evident at
520 higher blending ratios, which was mainly attributed to the higher amount of volatiles.

521 A novel synergy factor (SF), which showed a good correlation coefficient, was proposed to
522 quantify the synergistic effects and to distinguish catalytic effect from non-catalytic effect.
523 This index can be used as a tool to predict synergistic effect during co-processing, which is of
524 significant importance for optimizing blending ratio for existing boilers and for the design of
525 new co-firing plant to avoid operation issues. This index also offers opportunities for
526 selecting proper biomass for co-firing with poor quality coal to enhance the overall
527 combustion performance.

528 **Acknowledgement**

529 Part of this work was sponsored by Ningbo Bureau of Science and Technology under its Innovation
530 Team Scheme (2012B82011) and Major R&D Programme (2012B10042). The International Doctoral
531 Innovation Centre is also acknowledged for the provision of a full scholarship to the first author.

532 **References**

- 533 [1] Howaniec N, Smolinski A. Steam co-gasification of coal and biomass - Synergy in reactivity of
534 fuel blends chars. *Int J Hydrogen Energy*. 2013;16152 - 60.
- 535 [2] Chen X. Economic potential of biomass supply from crop residues in China. *Appl Energy*.
536 2016;166:141-9.
- 537 [3] De Laporte AV, Weersink AJ, McKenney DW. Effects of supply chain structure and biomass prices
538 on bioenergy feedstock supply. *Appl Energy*. 2016;183:1053-64.
- 539 [4] Li J, Brzdekiewicz A, Yang W, Blasiak W. Co-firing based on biomass torrefaction in a pulverized
540 coal boiler with aim of 100% fuel switching. *Applied Energy*. 2012;99:344-54.
- 541 [5] Nian V. The carbon neutrality of electricity generation from woody biomass and coal, a critical
542 comparative evaluation. *Appl Energy*. 2016;179:1069-80.
- 543 [6] Zhang Q, Li Q, Zhang L, Wang Z, Jing X, Yu Z, et al. Preliminary study on co-gasification behavior of
544 deoiled asphalt with coal and biomass. *Appl Energy*. 2014;132:426-34.
- 545 [7] Sahu SG, Chakraborty N, Sarkar P. Coal-biomass co-combustion: An overview. *Renewable and
546 Sustainable Energy Reviews*. 2014:575 - 86.
- 547 [8] Vamvuka D, Sfakiotakis S. Combustion behaviour of biomass fuels and their blends with lignite.
548 *Thermochim Acta*. 2011;526:192-9.
- 549 [9] Karampinis E, Nikolopoulos N, Nikolopoulos A, Grammelis P, Kakaras E. Numerical investigation
550 Greek lignite/cardoon co-firing in a tangentially fired furnace. *Appl Energy*. 2012;97:514-24.
- 551 [10] Lester E, Gong M, Thompson A. A method for source apportionment in biomass/coal blends
552 using thermogravimetric analysis. *J Anal Appl Pyrolysis*. 2007;80:111-7.
- 553 [11] Chen W-H, Wu J-S. An evaluation on rice husks and pulverized coal blends using a drop tube
554 furnace and a thermogravimetric analyzer for application to a blast furnace. *Energy*. 2009;34:1458-
555 66.
- 556 [12] Sjoström K, Chen G, Yu Q, Brage C, Rosen C. Promoted reactivity of char in co-gasification of
557 biomass and coal: synergies in the thermochemical process. *Fuel*. 1999:1189 - 94.
- 558 [13] Kastanaki E, Vamvuka D. A comparative reactivity and kinetic study on the combustion of coal -
559 biomass char blends. *Fuel*. 2006:1186-93.
- 560 [14] Rizkiana J, Guan G, Widayatno WB, Hao X, Huang W, Tsutsumi A, et al. Effect of biomass type on
561 the performance of cogasification of low rank coal with biomass at relatively low temperatures. *Fuel*.
562 2014:414-9.
- 563 [15] Van Lith SC, Jensen PA, Frandsen FJ, Glarborg P. Release to the Gas Phase of Inorganic Elements
564 during Wood Combustion. Part 2: Influence of Fuel Composition. *Energy & Fuels* 2008;22: 1598-609
- 565 [16] BS BS. *Solid Biofuels. Sample Preparation*. UK: BS; 2011.
- 566 [17] ISO IOFS. *Coal. Preparation of test samples Switzerland: ISO*; 2014.
- 567 [18] Yan J, Shi K, Pang C, Lester E, Wu T. Influence of minerals on the thermal processing of bamboo
568 with a suite of carbonaceous materials. *Fuel*. 2016;180:256-62.
- 569 [19] Wu T, Gong M, Lester E, Hall P. Characteristics and synergistic effects of co-firing of coal and
570 carbonaceous wastes. *Fuel*. 2013;104:194-200.
- 571 [20] Yan J, Shi K, Pang C, Lester E, Wu T. 2016;- 180:- 262.
- 572 [21] Pang CH, Gaddipatt S, Tucker G, Lester E, Wu T. Relationship between Thermal Behaviour of
573 Lignocellulosic Components and Properties of Biomass. *Bioresour Technol*. 2014;172:312-20.
- 574 [22] Wang C, Wang F, Yang Q, Liang R. Thermogravimetric studies of the behavior of wheat straw
575 with added coal during combustion. *Biomass Bioenergy*. 2009;33:50-6.

576 [23] Li X-g, Ma B-g, Xu L, Hu Z-w, Wang X-g. Thermogravimetric analysis of the co-combustion of the
577 blends with high ash coal and waste tyres. *Thermochim Acta*. 2006;441:79-83.

578 [24] Grote K-HA, EK;. Springer Handbook of Mechanical Engineering. New York: Springer Science &
579 Business Media; 2009.

580 [25] Ross AB, Jones JM, Cbaiklangmuang S, Pourkashanian M, Williams A, Kubica K, et al.
581 Measurement and Prediction of the Emissions of Pollutants from the Combustion in a Fixed Bed
582 Furnace. *Fuel*. 2002:571 - 852.

583 [26] Tchapda AH, Pisupati SV. A Review of Thermal Co-Conversion of Coal and Biomass/Waste.
584 *Energies*. 2014:1098-148.

585 [27] Shao Y, Wang J, Xu C, Zhu J, Preto F, Tourigny G, et al. An experimental and modeling study of
586 ash deposition behaviour for co-firing peat with lignite. *Appl Energy*. 2011;88:2635-40.

587 [28] Habibi R, Kopyscinski J, Masnadi MS, Lam J, Grace JR, Mims CA, et al. Co-gasification of biomass
588 and non-biomass feedstocks: Synergistic and inhibition effects of switchgrass mixed with sub-
589 bituminous coal and fluid coke during CO₂ gasification. *Energy Fuels*. 2012:494–500.

590 [29] Akram M, Tan CK, Garwood DR, Fisher M, Gent DR, Kaye WG. Co-firing of pressed sugar beet
591 pulp with coal in a laboratory-scale fluidised bed combustor. *Appl Energy*. 2015;139:1-8.

592 [30] Avila C, Pang CH, Wu T, Lester E. Morphology and reactivity characteristics of char biomass
593 particles. *Bioresour Technol*. 2011;102:5237-43.

594 [31] Nowakowski DJ, Jones JM, Brydson RMD, Ross AB. Potassium catalysis in the pyrolysis behaviour
595 of short rotation willow coppice. *Fuel*. 2007;86:2389-402.

596 [32] Zheng GK, JA;. Thermal events occurring during the combustion of biomass residue. *Fuel*.
597 2000:181-92.

598 [33] Xiao H-m, Ma X-q, Lai Z-y. Isoconversional kinetic analysis of co-combustion of sewage sludge
599 with straw and coal. *Appl Energy*. 2009;86:1741-5.

600 [34] Vamvuka D, El Chatib N, Sfakiotakis S. Measurements of Ignition Point and Combustion
601 Characteristics of Biomass Fuels and their Blends with Lignite. Combustion Institute 2011.

602 [35] Haykiri-Acma H, Yaman S. Effect of co-combustion on the burnout of lignite/biomass blends: A
603 Turkish case study. *Waste Manage*. 2008;28:2077-84.

604 [36] Aboulkas A, El harfi K, El bouadili A, Nadifiyine M, Benchanaa M, Mokhlisse A. Pyrolysis kinetics
605 of olive residue/plastic mixtures by non-isothermal thermogravimetry. *Fuel Process Technol*.
606 2009;90:722-8.

607 [37] Abreu P, Casaca C, Costa M. Ash deposition during the co-firing of bituminous coal with pine
608 sawdust and olive stones in a laboratory furnace. *Fuel*. 2010;89:4040-8.

609 [38] Kreckkaiwan S, Fushimi C, Tsutsumi A, Kuchonthara P. Synergetic effect during co-pyrolysis /
610 gasification of biomass and sub-bituminous coal. *Fuel Processing Technology*. 2013:11-6.

611 [39] Adeyemi I, Janajreh I, Arink T, Ghenai C. Gasification behavior of coal and woody biomass:
612 Validation and parametrical study. *Appl Energy*. 2016.

613 [40] Zhang L, Xu SP, Zhao W, Liu SQ. Co-pyrolysis of biomass and coal in a free fall reactor. *Fuel*
614 2007:353–9.

615 [41] Straka P, Nahunkova J, Brozova Z. Kinetics of copyrolysis of coal with polyamide 6. *J Anal Appl*
616 *Pyrolysis*. 2004:213-21.

617 [42] Sonobe T, Worasuwannarak N, Pipatmanomai S. Synergies in co-pyrolysis of Thai lignite and
618 corncob. 2008:1371 - 8.

619 [43] Kumabe K, Hanaoka T, Fujimoto S, Minowa T, Sakanishi K. Co-gasification of woody biomass and
620 coal with air and steam. *Fuel*. 2007:684–9.

621 [44] Kazagic A, Smajevic I. Synergy effects of co-firing wooden biomass with Bosnian coal. *Energy*.
622 2009;34:699-707.

623 [45] Haykiri-Acma H. Combustion characteristics of different biomass materials. *Energy Convers*
624 *Manage*. 2003;44:155-62.

625 [46] Li XG, Lv Y, Ma BG, Jian SW, Tan HB. Thermogravimetric investigation on co-combustion
626 characteristics of tobacco residue and high-ash anthracite coal. *Bioresour Technol*. 2011;102:9783-7.

- 627 [47] Şentorun Ç, Küçükbayrak S. Effect of mineral matter on the burning profile of lignites.
628 Thermochem Acta. 1996;285:35-46.
- 629 [48] Zhang Y, Zheng Y, Yang M, Song Y. Effect of fuel origin on synergy during co-gasification of
630 biomass and coal in CO₂. Bioresour Technol. 2016;200:789-94.
- 631 [49] Shi KW, Tao; Yan, Jiefeng; et al. Thermogravimetric Studies on Co-combustion Characteristics of
632 Mengxi Coal and Poplar. Switzerland: Springer; 2014.
- 633 [50] Parvez AM, Wu T. Characteristics and interactions between coal and carbonaceous wastes
634 during co-combustion. J of Energy Inst.

635

636